

Band Gap Engineering and Frequency Dispersive Dielectric Properties of Rare Earth (Sm^{3+}) Modified $\text{Ba}_{0.8}\text{Sr}_{0.2}\text{TiO}_3$ Ceramics for Potential Use as an Optoelectronic Materials

Jyotirekha Mallick and Manoranjan Kar*

Department of Physics, Indian Institute of Technology Patna, Bihta, Bihar-801106, India

Volume 1, Issue 5, October 2024

Received: 30 July, 2024; Accepted: 29 October, 2024

DOI: <https://doi.org/10.63015/5C-2434.1.5>

*Correspondence Author Email: mano@iitp.ac.in

Abstract: Lead free perovskite materials have the capability to be used in various multifunctional applications. In this regard, dielectric and light absorption properties of Sm modified $\text{Ba}_{0.8-x}\text{Sm}_x\text{Sr}_{0.2}\text{TiO}_3$ have been explored. The dielectric constant has been estimated to be 2788 for $\text{Ba}_{0.77}\text{Sm}_{0.03}\text{Sr}_{0.2}\text{TiO}_3$. The optical band gap of all prepared samples has been evaluated by employing Tauc plot method and observed that the band gap varies 3.13-2.97 eV with the increase in Sm concentration. In brief, the present study reports the physical properties of $\text{Ba}_{0.8-x}\text{Sm}_x\text{Sr}_{0.2}\text{TiO}_3$ ceramics which open window for possible use of it as lead-free optoelectronic material.

Keywords: Perovskite materials, Dielectric constant, Optoelectronic, Band gap

1. Introduction: Recently, the importance of the lead-free perovskite materials in the electronic industries has gained significant attention because of their rapid development in various technologies such as sensor, light emitting diode, dielectric capacitors as well as commitment to environment protection [1,2]. These materials can also enhance/change their physical properties when expose to light and considered as a potential candidate to be used in photovoltaic devices. So researchers are very much interested to understand the light matter interaction and investigate its various applications such as photodetector, photovoltaic devices, etc. [3-5]. Among all lead-free perovskite materials, Barium titanate (BaTiO_3) has earned so much attention of researchers due to its excellent dielectric, ferroelectric, piezoelectric properties. BaTiO_3 belongs to ABO_3 type structure, with Ba^{2+} and Ti^{4+} are placed at the A and B-site, respectively, within the octahedral co-ordination of oxygen atoms, hence possesses unique ferroelectric properties [6]. Most importantly it also exhibits significant optical

properties and become suitable to be utilized in different electro-optical system. Optoelectronic devices play an important role to produce various materials for advanced electronic equipment. For example, rare earth ions have an empty and entangled 4f electron structure which has capability to enhance various physical properties. Previously, Tihtih. M et. al. reported that rare earth modified BTO system can improve the materials optical properties and expand its potentiality in different technological applications [7]. Also, by the addition of lower ionic radii element, such as Sr^{2+} at A site of BTO system stabilizes the perovskite structure and noticeably enhance the dielectric constant [8]. Hence, $\text{Ba}_{0.8}\text{Sr}_{0.2}\text{TiO}_3$ (BSTO) is the one of the most important member of the BaTiO_3 family which has achieved a lot of attention from the researchers due to its high dielectric constant with diffuse phase transition behaviour [8]. With the increase in Sr^{2+} in BaTiO_3 the relaxor behaviour of BSTO increases and it exhibits better relaxor ferroelectric when the concentration of Sr^{2+} is 20% as compared to

other compositions [8]. That's why BSTO has been chosen to be substitute rare earth element at Ba site. The introduction of rare earth elements (Re^{3+}) at the Ba site of BSTO can significantly enhanced the physical properties of the modified BSTO by inducing structural deformation of octahedra as well as modifies the lattice symmetry [9]. Basically, the ionic radius of the rare earth element (trivalent element) varies between 0.8 and 1.13 Å which are suitable to be placed at the Ba^{2+} site of the ABO_3 structure. So it is the most crucial work to choose the perfect rare earth element which can produce better dielectric constant with low dielectric loss as well as induced low optical band gap of modified BTO system [10]. It has been observed that the dielectric constant, transition temperature and electrical resistance can be controlled strongly by the proper addition of donor impurity ions at the A site of BTO [11]. Thakur and their group observed that by the substitution of Sm^{3+} at the Ba^{2+} site can enhance the dielectric constant at room temperature [12]. The microstructure and dielectric properties of rare earth (Sm, Ho, Yb), modified BaTiO_3 has been investigated by Jo et. al. and they concluded that the unit cell volume of rare earth doped BTO plays an important role in the regulation of Curie temperature [13]. In this context the Sm^{3+} substituted $\text{Ba}_{0.8-x}\text{Sm}_x\text{Sr}_{0.2}\text{TiO}_3$ were prepared and their crystal structure, temperature dependent dielectric and electrocaloric properties were reported by the present authors [14]. However, the frequency dependent dielectric constant is important to explore for the technological application. As well as these materials are very promising for the optoelectronic application as their optical band gap is around 3 eV. Hence, in this article the frequency dependent dielectric constant and band gap engineering by Sm substitution in BSTO have been explored. The present article will guide the researcher for further modification of band gap of BTO for its technological applications.

2. Experimental details: Polycrystalline ceramics $\text{Ba}_{0.8-x}\text{Sm}_x\text{Sr}_{0.2}\text{TiO}_3$ ($x = 0.01 \leq x \leq 0.05$) were prepared by employing the

conventional high temperature solid-state reaction method. Previously, the sample preparation method, characterization, temperature dependent dielectric, ferroelectric and electrocaloric effect properties are reported elaborately in the author's previous publication [14]. For the present study, the N4L impedance analyser has been used to measure the room temperature complex impedance spectroscopy within the frequency range 1Hz-1MHz. The UV visible Shimadzu UV-2600 spectrophotometer (Japan) has been employed to record the diffuse reflectance spectra for exploring the optical properties of all the prepared samples.

3. Results and discussion

3.1 Crystal structure and structural properties: The XRD patterns of Polycrystalline ceramics $\text{Ba}_{0.8-x}\text{Sm}_x\text{Sr}_{0.2}\text{TiO}_3$ ($x = 0.01, 0.02, 0.03, 0.04$ and 0.05) as previously reported confirm that all the sample have good crystallinity without any impurity [14]. All samples are belonging to tetragonal symmetry with $P4mm$ space group. Also all sintered pellets are exhibited a dense and compact surface morphology which is an important factor in the improvement of different physical properties. The temperature dependent dielectric properties, ferroelectric and electrocaloric properties are reported as discussed in the introduction [14]. However, in this article, the frequency dependent dielectric constant and optical band gap properties are discussed.

3.2. Dielectric Properties

3.2.1. Dielectric constant: Room temperature dielectric constant as function of frequency of $\text{Ba}_{0.8-x}\text{Sm}_x\text{Sr}_{0.2}\text{TiO}_3$ ($x = 0.01, 0.02, 0.03, 0.04$, and 0.05) are represented in the Figure 1(a). Basically, the dielectric constant of a ceramic involves different types of polarization such as ionic, dipolar, electronic, and interfacial. Depending upon the relaxation time, their

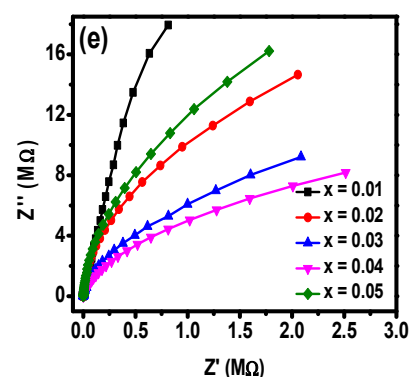
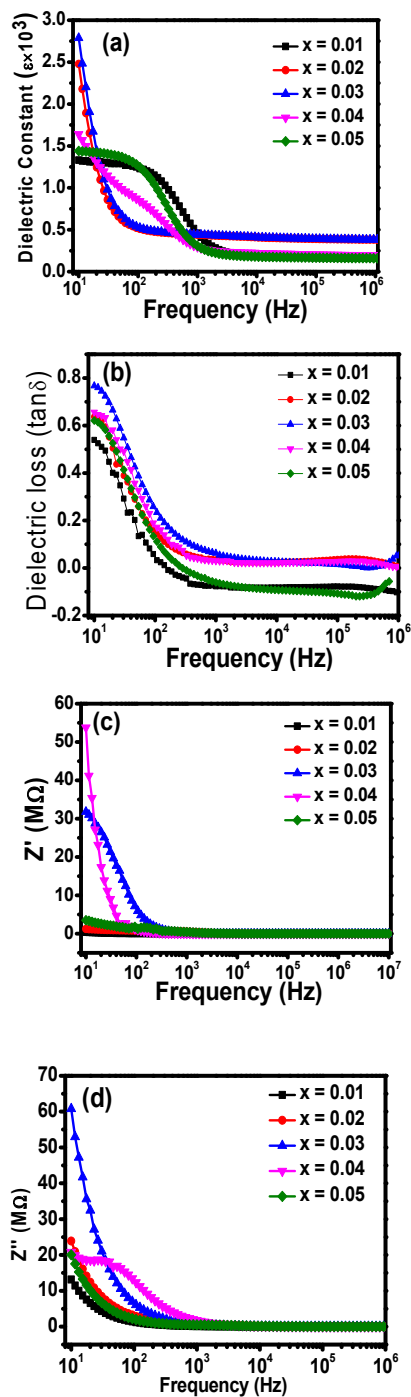


Figure-1: Room temperature frequency variation (a) dielectric constant, (b) tanloss, (c) real and (d) imaginary part of impedance, (e) Cole – Cole plots of $\text{Ba}_{0.8-x}\text{Sm}_x\text{Sr}_{0.2}\text{TiO}_3$ ($x = 0.01, 0.02, 0.3, 0.04$ and 0.05) compounds.

contribution varies from lower frequency to higher frequency. It is clearly noticed from the Figure 1(a) that there is the reduction of dielectric constant value with the increase in frequency but at higher frequency it becomes constant. Hence it is concluded that all the prepared samples possess dielectric dispersion behaviour. This dispersion behaviour can be clearly understood by employing Maxwell Wagner model along with the Koops phenomenological theory [15].

Basically, at lower frequency, there is the accumulation of charges at the grain boundary along the applied field, produce large polarization and enhance the value of dielectric constant. But at higher frequency, the molecular dipoles are not able to orient along the direction of applied field, hence the probability of dipoles to be reached at the grain boundary is less, so it produces low polarization as well as low dielectric constant. The maximum dielectric constant is estimated to be 2788 for $\text{Ba}_{0.77}\text{Sm}_{0.03}\text{Sr}_{0.2}\text{TiO}_3$ ceramic. Also, this dielectric constant value increases with the Sm^{3+} concentration up to $x = 0.03$, after that it diminishes. The c/a ratio i.e. tetragonality is mainly responsible for this behaviour. With the increase in Sm^{3+} concentration the tetragonality behaviour of the sample increases up to $x = 0.03$ which enhances spontaneous polarization as well as

the dielectric constant value increases [14]. But when the concentration value is more than 0.03, there might be production of oxygen vacancies because of the replacement of Sm^{3+} at Ba^{2+} site. These oxygen vacancies can oppose the orientation of dipoles and inhibits the increase of dielectric constant, when the concentration of Sm^{3+} is more than $x = 0.03$.

3.2.2. Dielectric loss: Dielectric loss as a function of frequency of all the prepared samples is shown in Figure 1(b). It decreases with increase in frequency and at higher frequency range, dielectric loss become constant, which can also be understood by Maxwell Wagner model [14]. The Maxwell Wagner model describes that a dielectric material made up of a semiconducting grain enclosed by highly insulating grain boundary. At low frequency, insulating grain boundaries are active, so accumulation of charge carriers increases. Hence more energy is required to transport the charge carriers through the grain boundary and produce high dielectric loss. But at high frequency, semiconducting grains are more active so charge carriers can easily pass through the grain without loss of more energy and produce low dielectric loss. Hence, this characterization indicates the lossless behaviour of the prepared sample and depict that these samples have the capability to be used in the devices which are operated at high frequency.

3.2.3. Complex Impedance spectroscopy:

The real (Z') and imaginary (Z'') part of ac impedance as a function of frequency for all the prepared samples $\text{Ba}_{0.8-x}\text{Sm}_x\text{Sr}_{0.2}\text{TiO}_3$ ($0.01 \leq x \leq 0.05$) are represented in Figures 1(c) and 1(d). Figure 1(c) confirmed that Real (Z') part of impedance decreases with the increase in frequency and become frequency independent at higher frequency. At low frequency, all types of polarizations are contributed towards total impedance hence the value of Z' is high. The imaginary (Z'') part of ac impedance is also exhibit similar types of behaviour. The dielectric properties of ceramic materials over a broad range of frequency can be understood properly by Complex

Impedance Spectroscopy (CIS) technique. Figure 1(e) represents the Cole-Cole plot of all the samples. The total impedance is the contribution of grain, grain boundary, and electrodes. Figure 1(e) represents a semicircle arc bend towards the X axis, which confirm that the contribution of grain is dominated over the grain boundary and electrodes.

3.3. Optical Properties: The optical properties of $\text{Ba}_{0.8-x}\text{Sm}_x\text{Sr}_{0.2}\text{TiO}_3$ ($x = 0.01, 0.02, 0.03, 0.04, \text{ and } 0.05$) have been discussed by using UV visible spectrometer in the range of (200 – 1000) nm as represented in the Figure 2.

The optical band gap energy (E_g) has been estimated by employing the Kubelka and Munk function. The KM function [$F(R_\infty)$] is [15]:

$$F(R_\infty) = \frac{(1-R_\infty)^2}{2R_\infty} = \frac{\alpha}{s} \quad (1)$$

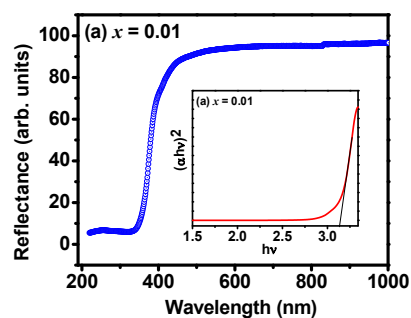
Where, α , R_∞ , and s denote absorbance coefficient, the reflectance of the ceramics, and scattering coefficient, respectively.

So, the KM function is influence by the absorption spectrum. The absorption coefficient (α) as a function of energy can be represented as [15];

$$\alpha \propto \left[\frac{(h\nu - E_g)^n}{h\nu} \right] \quad (2)$$

The Tauc's method has been used to calculate the optical band gap of prepared ceramics,

$$\alpha h\nu = A(h\nu - E_g)^n \quad (3)$$



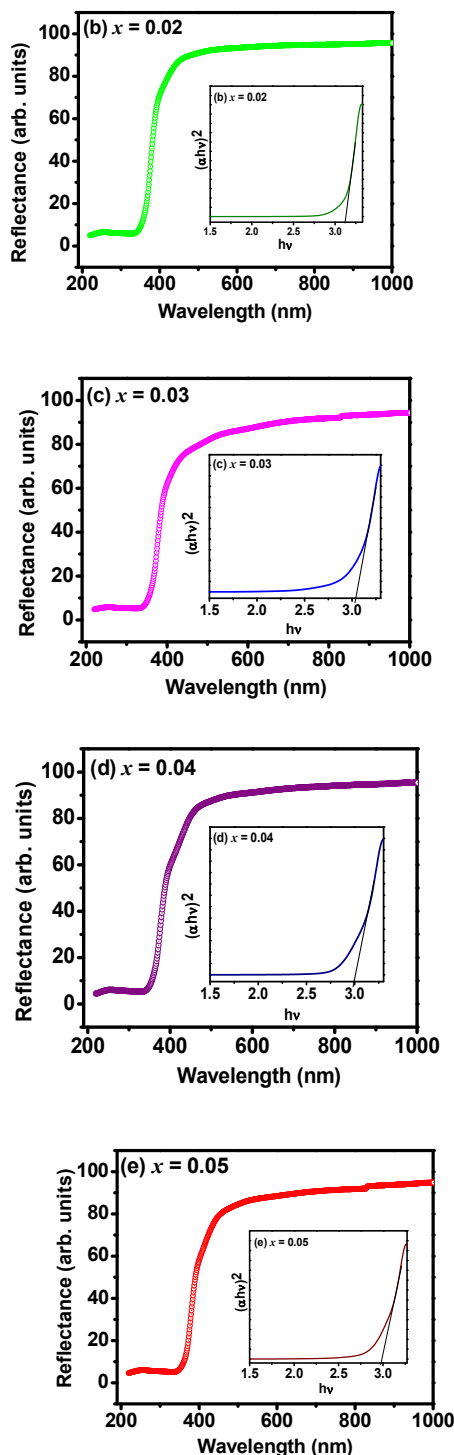


Figure 2: UV visible diffuse reflectance spectra and Tauc plots (inset in the Figure) of $\text{Ba}_{0.8-x}\text{Sm}_x\text{Sr}_{0.2}\text{TiO}_3$ for (a) $x = 0.01$, (b) $x = 0.02$, (c) $x = 0.03$, (d) $x = 0.04$, and (e) $x = 0.05$.

Here, A , $h\nu$, E_g , n and α represent a constant, photon energy, optical band gap, a

constant related to different types of electronic transition and absorbance, respectively. The value of n is different for different types of transition such as $n = 1/2, 2, 3/2$, and 3 for direct allowed transition, indirect allowed transition, directly forbidden, and indirect forbidden, respectively.

Here, $\text{Ba}_{0.8-x}\text{Sm}_x\text{Sr}_{0.2}\text{TiO}_3$ is considered as direct band gap. Hence, $(\alpha h\nu)^2$ vs. $h\nu$ have been plotted and shown in the Figure 2 (inset figure). The optical band gap has been estimated by extrapolating the tangent of the curves that intersects the $h\nu$ -axis directly and gives the optical band gap of the samples. The obtained band gaps are 3.13, 3.12, 3.03, 2.99 and 2.97 eV for $x = 0.01, 0.02, 0.03, 0.04$, and 0.05 , respectively. One can noticed that the optical energy gap decreases with the Sm^{3+} concentration, this is due to the structural disorder induced in the lattice because of the formation of A-site vacancies and distortions in the octahedral clusters (TiO_6). This A-site vacancy creates shallow defects in the band gap of BSTO and decreases its value. So with increase in Sm^{3+} concentration, the A-site vacancies increase as well as increases the shallow defects and distortion in TiO_6 octahedron [16]. Hence optical band gap decreases with further increase in Sm^{3+} concentration. Overall, the formation of shallow defects is the reason behind the optical characteristics of $\text{Ba}_{0.8-x}\text{Sr}_{0.2}\text{Sm}_x\text{TiO}_3$.

4. Conclusion: Incorporation of Sm^{3+} plays an important role in the reduction of dielectric constant in BSTO. The highest dielectric constant value is found to 2788 for $\text{Ba}_{0.77}\text{Sm}_{0.03}\text{Sr}_{0.2}\text{TiO}_3$. The estimated optical band gap of Sm^{3+} modified BSTO is varies between (3.13-2.97) eV. This is basically because of the new electronic levels in the BSTO band gap due to the Sm^{3+} addition to its lattice site. These electronic levels modify the conduction band and make a continuous band by lowering the band gap. Overall, the above discussion indicates that the Sm^{3+} substituted BSTO has the potential to be used in different applications mainly in optoelectronic devices.

Acknowledgements

The authors acknowledge the support from the UGC-DAE CSR project (Project No. CRS/2021-22/03/595).

References

- [1] J.F. Li, K. Wang, F.Y. Zhu, L.Q. Cheng, F.Z. Yao, (K,Na)NbO₃-Based lead-free piezoceramics: fundamental aspects, processing technologies, and remaining challenges, *J. Am. Ceram. Soc.* 96 (2013) 3677–3696.
- [2] J. Wu, D. Xiao, J. Zhu, Potassium–sodium niobate lead-free piezoelectric materials: past, present, and future of phase boundaries, *Chemi. Rev.* 115 (2015) 2559–2595.
- [3] Feteira, D. C. Sinclair, I. M. Reaney, Y. Somiya, and M. T. Lanagan BaTiO₃-based ceramics for tunable microwave applications *J. Am. Ceram. Soc.* **87**, 1082–7(2004).
- [4] B. Wang, Z. Huang, P. Tang, S. Luo, Y. Liu, J. Li, X. Qi, One-pot synthesized Bi₂Te₃/ graphene for a self-powered photoelectrochemical-type photodetector, *Nanotechnology* 31 115201(2020).
- [5] J. Zhang, S. Jiao, D. Wang, S. Ni, S. Gao, J. Wang, Solar-blind ultraviolet photodetection of an α -Ga₂O₃ nanorod array based on photoelectrochemical selfpowered detectors with a simple, newly-designed structure, *J. Mater. Chem. C.* 7 6867–6871(2019).
- [6] K.M. Sangwan, N. Ahlawat, R. Kundu, S. Rani, S. Rani, N. Ahlawat, S. Murugavel, Improved dielectric and ferroelectric properties of Mn doped barium zirconium titanate (BZT) ceramics for energy storage applications, *J. Phys. Chem. Solid.* 117 (2018) 158–166.
- [7] M. Tihiti, J.E.F. Ibrahim, M.A. Basyooni, R. En-Nadir, I. Hussainova, I. Kocserha, Functionality and activity of sol-gel-prepared Co and Fe co-doped lead-free BTO for thermo-optical applications, *ACS Omega* 8 (2023) 5003–5016.
- [8] Mallick, J., Manglam, M. K., Pradhan, L. K., Panda, S. K., & Kar, M. (2022). Electrocaloric effect and temperature dependent scaling behaviour of dynamic ferroelectric hysteresis studies on modified BTO. *Journal of Physics and Chemistry of Solids*, 169, 110844.
- [9] J.Q. Qi, B.B. Liu, H.Y. Tian, H. Zou, Z.X. Yue, L.T. Li, Dielectric properties of barium zirconate titanate (BZT) ceramics tailored by different donors for high voltage applications, *Solid State Sci.* 14 (2012) 1520–1524.
- [10] E.H. Yahakoub, A. Bendahhou, K. Chourti, F. Chaou, I. Jalafi, S. El Barkany, Z. Bahari, M. Abou-salama, Structural, electrical, and dielectric study of the influence of 3.4% lanthanide (Ln³⁺ = Sm³⁺ and La³⁺) insertion in the A-site of perovskite Ba_{0.95}Ln_{0.034}Ti_{0.99}Zr_{0.01}O₃, *RSC Adv.* 12 (2022) 33124–33141
- [11] S. Garcia, R. Font, J. Portelles, R.J. Quinones, J. Heiras, J.M. Siqueiros, “Effect of Nb Doping on (Sr,Ba)TiO₃ (BST) Ceramic Samples, *J. Electroceram.*” **6**, 101 (2001).
- [12] O.P. Thakur and C. Prakash, Dielectric Properties of Samarium Substituted Barium Strontium Titanate, *Phase Transitions*, **76**, 567-574 (2003).
- [13] S. K. Jo, J. S. Park, and Y. H. Han, “Effects of multi-doping of rare-earth oxides on the microstructure and dielectric properties of BaTiO₃,” *Jour. of Alloys and Compds.* **501**, 259–264 (2010).
- [14] Mallick, J., Shukla, A., Panda, S. K., Manglam, M. K., Biswal, S. K., Pradhan, L. K., & Kar, M. (2023). Enhanced ferroelectricity and electrocaloric effect of Sm modified BSTO with temperature stability near room temperature. *Journal of Applied Physics*, 133(6).
- [15] Mallick, J., Shukla, A., Panda, S. K., Biswal, S. K., Rout, S. N., Yadav, M. K., & Kar, M. (2024). Crystal symmetry transition and its influence on optical, dielectric, and ferroelectric properties in (1-x) Na_{0.5}Bi_{0.5}TiO₃-xSrTiO₃ system. *Journal of Alloys and Compounds*, 978, 173403.
- [16] Ganguly, M.; Rout, S.K. ; Woo, W.S. ; Ahn, C.W.; Kim, I.W.; *Phys. B Condens. Matter* **2013**, **411**, 26–34.